Applied and Environmental Microbiology, Oct. 2008, p. 6437–6443 Vol. 74, No. 20
0099-2240/08/$08.00+0 doi:10.1128/AEM.01194-08

Characterization and Deposition of Respirable Large- and Small-Particle Bioaerosols[▽]

Richard J. Thomas,[1]* Daniel Webber,[1] William Sellors,[1] Aaron Collinge,[1] Andrew Frost,[1] Anthony J. Stagg,[1] Stephen C. Bailey,[1] Pramukh N. Jayasekera,[1] Rosa R. Taylor,[1] Steve Eley,[1] and Richard W. Titball[2]

Defence Science and Technology Laboratory (Dstl), Porton Down, Salisbury, Wiltshire SP4 0JQ, United Kingdom,[1] and School of Biosciences, Geoffrey Pope Building, University of Exeter, Exeter, Devon EX4 4QU, United Kingdom[2]

Received 29 May 2008/Accepted 12 August 2008

The deposition patterns of large-particle microbiological aerosols within the respiratory tract are not well characterized. A novel system (the flow-focusing aerosol generator [FFAG]) which enables the generation of large (>10-μm) aerosol particles containing microorganisms under laboratory conditions was characterized to permit determination of deposition profiles within the murine respiratory tract. Unlike other systems for generating large aerosol particles, the FFAG is compatible with microbiological containment and the inhalational challenge of animals. By use of entrapped *Escherichia coli* cells, *Bacillus atrophaeus* spores, or FluoSphere beads, the properties of aerosols generated by the FFAG were compared with the properties of aerosols generated using the commonly available Collison nebulizer, which preferentially generates small (1- to 3-μm) aerosol particles. More entrapped particulates (15.9- to 19.2-fold) were incorporated into 9- to 17-μm particles generated by the FFAG than by the Collison nebulizer. The 1- to 3-μm particles generated by the Collison nebulizer were more likely to contain a particulate than those generated by the FFAG. *E. coli* cells aerosolized using the FFAG survived better than those aerosolized using the Collison nebulizer. Aerosols generated by the Collison nebulizer and the FFAG preferentially deposited in the lungs and nasal passages of the murine respiratory tract, respectively. However, significant deposition of material also occurred in the gastrointestinal tract after inhalation of both the small (89.7%)- and large (61.5%)-particle aerosols. The aerosols generated by the Collison nebulizer and the FFAG differ with respect to mass distribution, distribution of the entrapped particulates, bacterial survival, and deposition within the murine respiratory tract.

Environmental bioaerosols can have a profound influence on human health, due to infectious disease, hypersensitivity conditions (e.g., hay fever), and acute inflammatory responses resulting from the inhalation of irritants. Environmental aerosols comprise a polydisperse distribution composed of a range of particle sizes from submicron to large droplets thousands of microns in diameter. Hence, such aerosols contain a proportion of particles of >10 μm, herein defined as "large particles." Indeed, analysis of the particle sizes containing bacteria within the atmosphere indicated that ~40% are greater than 7 μm, due to adherence to debris (27). Environmental microbial aerosols can arise from a number of sources, including food processing (13, 19, 40); water sources, e.g., contaminated air conditioning systems, shower heads, water faucets, and cooling towers (2, 42, 53); pesticide sprayers (1); and fungal-spore generation (15, 26). The importance of bioaerosols from a civilian biodefense perspective was highlighted by the U.S. anthrax mail attacks in 2001 (3).

In health care settings, nosocomial transmission may occur by patients coughing or sneezing, generating respirable particles within the diameter range of 0.5 to 12 μm (6, 14); alternatively, pathogens can be reaerosolized after previous deposition on surfaces (46). Several important human and veterinary pathogens are transmitted by contaminated respiratory droplets (8, 46, 47). Evaporation of water from large respiratory particles results in the generation of smaller particles comprising the dried components, such as microbial biomass and mucin (37, 51). The rate of evaporation is dependent on the relative humidity (RH) and temperature of the air, air turbulence, and the constituents of the particle. The quantity of nonvolatile material within particles of >20 μm results in particles larger than 5 μm (37).

Particle size influences the site of deposition in the respiratory tract within humans and animals (21, 24, 29, 41, 45) and survival of the microbe in the aerosol (28, 50) and determines the length of time aerosolized microorganisms remain suspended within the atmosphere (25). Small particles around the size of a bacterium (1 to 5 μm) deposit in the alveoli, while larger particles (>10 μm) deposit in the upper respiratory tract (URT) (36, 41, 45). The importance of particle size to infection, microbial survival, and deposition is clear; however, the ability to assess bioaerosols with respect to particle size under defined experimental conditions is limited. Historically, the Collison nebulizer has been used to generate small-particle aerosols with a mass median aerodynamic diameter (MMAD) of 1 to 3 μm for animal exposure studies (34). Aerosols with particles greater than 10 μm have been produced by a spinning-top aerosol generator (STAG) connected to a drying column (9, 10, 11, 12, 21, 43). However, this method is difficult to carry out in microbiological containment facilities created for

* Corresponding author. Mailing address: Defence Science and Technology Laboratory (Dstl), Porton Down, Salisbury, Wiltshire SP4 0JQ, United Kingdom. Phone: 44 (01980) 613199. Fax: 44 (01980) 614307. E-mail: rjthomas@dstl.gov.uk.

▽ Published ahead of print on 22 August 2008.

animal exposure studies. Alternative methods for generating large-particle aerosols would be beneficial.

Recently, a novel flow-focusing method of generating large-particle aerosols has been developed (17). Liquid is pumped through a capillary needle of defined diameter and drawn through a critical orifice. Upon application of an appropriate pressure from a compressed air supply, the focused liquid splits into particles of a defined size at a specific distance from the orifice of the aerosol generator. The orifice diameter is fixed; however, upon modulation of the liquid flow rate or gas pressure, particle sizes greater than 10 μm can be generated. The aerosols are produced with a geometric standard deviation (GSD) of 1.1 to 1.3, indicating particle uniformity (16, 17, 31). An important distinction between the two methods is the generation of wet and dry particles by the flow-focusing aerosol generator (FFAG) and the STAG, respectively. This technique may be applicable to the generation of large-particle aerosols containing microbiological material.

This study aimed to characterize 12-μm large-particle aerosols produced by the FFAG with respect to MMAD, particulate distribution within the particles (*Escherichia coli* cells, *Bacillus atrophaeus* spores, and fluospheres), bacterial survival, and deposition and clearance of the aerosols within the murine respiratory and gastrointestinal (GI) tracts. Comparisons with the Collison nebulizer, a device commonly used to produce small-particle microbiological aerosols for pneumonic models of disease in biodefense and health care research, are made.

MATERIALS AND METHODS

Bacterial strains. *E. coli* MRE162 and *B. atrophaeus* (formerly *B. globigii* and *B. subtilis* var. *niger*) spores were obtained from the in-house culture collection at Dstl Porton Down. *E. coli* MRE162 was routinely cultured on LB agar plates at 37°C for 24 h for the isolation of single colonies. For aerosol exposures, nutrient broth cultures were shaken at 120 rpm for 24 h at 37°C, producing a concentration of $1.0 \times 10^9 \pm 0.36 \times 10^9$ CFU ml^{-1}. Stock cultures were maintained at −80°C in nutrient broth containing 10% (vol/vol) glycerol. *B. atrophaeus* spores were prepared from a stock held at a concentration of 5×10^9 spores ml^{-1}. The spores were washed twice in distilled water, with centrifugation (13,000 × *g*). The spores were resuspended to a concentration of 1.0×10^9 CFU ml^{-1} and heat treated at 70°C for 30 min to remove vegetative cells. Enumeration was done by serial dilution and plating onto tryptic soy agar plates; the resultant suspension was then stored at 4°C.

Animals. Female BALB/c mice (Charles River, United Kingdom) were used during the study and housed with free access to pelleted food and water within a rigid unplasticized polyvinylchloride (PVCu) fixed-film isolator at biological safety level 3 (BSL-3). The mice supplied for aerosol exposure studies were 6 to 8 weeks old and 20 to 25 g in weight. All mice were permitted to acclimatize for 1 week prior to any procedures. All procedures were performed in strict accordance with the Scientific Procedures (Animals) Act of 1986.

Aerosol generation and sampling. The particulates comprised *E. coli* cells, *B. atrophaeus* spores (prepared as described above), or fluospheres (diameter of 1.1 ± 0.035 μm, volume of 0.697 μm^3; Molecular Probes, Inc.) diluted to a concentration of 10^9 ml^{-1}. Aerosol samples were collected for 1 min into an all-glass impinger (AGI-30; Ace Glass Inc., NJ) containing 10 ml of phosphate-buffered saline (PBS) at a flow rate of 12 liters min^{-1}. The impinger samples were serially diluted and plated onto agar for enumeration as previously described (32). The small-particle aerosols were generated using a three-jet Collison nebulizer (13.5-μm-diameter jet holes) at a pressure of 26 lb/in^2 (179,000 Pa) (34). For animal exposures, the Collison nebulizer spray was mixed with a secondary air supply of controlled RH of 45 to 50% within a Henderson apparatus (23) contained within a rigid PVCu half-suit isolator with a stainless steel base (Howorth Airtech Ltd., United Kingdom) at BSL-3. At 45 to 50% RH, predominantly 1-μm particles containing single microorganisms are generated (34). The total flow rate through the Henderson apparatus was 66 liters min^{-1}. The large-particle aerosols were generated using an FFAG (75-μm-diameter orifice) purchased from Ingeniatrics Tecnologías (Seville, Spain). Tubing and connections were purchased from VWR International, United Kingdom. The FFAG relies on the formation of a stable microjet that disintegrates at a defined distance from a critical orifice (16, 17). For the generation of 12-μm particles, the system was operated at a pressure of 16 lb/in^2 (110,000 Pa) derived from a filtered compressed air supply and the liquid supplied via a syringe pump (model 11 Plus advanced pump; Harvard Apparatus, United Kingdom) at a flow rate of 50 μl min^{-1}. The generation of 12-μm particles for animal exposure studies was performed under operation at BSL-3. The parameters used while operating the FFAG are described above. In addition, air was mixed from a secondary air supply of controlled RH at 65 to 70% derived from the Henderson apparatus to prevent evaporation of the large particles. An elevated RH of 65 to 70% was used to ensure that evaporation of the 12-μm particles did not occur. The particle size distribution was determined by use of a Grimm no. 107 environmental dust monitor (Grimm Aerosol Technik GmbH & Co., Germany), which utilizes orthogonal laser light scattering at a 90° angle. The measurement range for particles was from 0.25 to >32 μm. Particle counts ranged from 1.0×10^6 to 2.0×10^6 liter^{-1}. The aerosol was continuously sampled at a flow rate of 72 liter h^{-1}, with the number and size of particles measured each minute. The aerosols generated are described by the MMAD, which is the particle diameter that halves the mass distribution; the GSD, which provides a representation of the uniformity of the particles and is obtained by dividing the MMAD by the particle size at either the 15.78% or the 84.13% probability; and the particle sizes below which 10% or 90% of the total particles produced in the aerosol occur.

Characterization of particulate distribution. *E. coli* and *B. atrophaeus* spores were chosen as representative gram-negative vegetative cells and gram-positive spores, respectively. Fluospheres (diameter of 1.1 ± 0.035 μm; volume of 0.697 μm^3) possess dimensions similar to those of bacteria and were used as surrogate bacterial particulates. Bacteria or spores were prepared and enumerated as described above before dilution with PBS to a final concentration of 10^9 ml^{-1}. The bacterium or spore preparations were labeled with 1 mg ml^{-1} fluorescein isothiocyanate (FITC) (Sigma-Aldrich Ltd., United Kingdom) for 24 h at 4°C. Excess FITC was removed by multiple washes in distilled water with centrifugation steps (13,000 × *g*) until the supernatant was clear. The *E. coli* cells, spores, or yellow fluospheres were diluted with distilled water to a final concentration of 10^9 ml^{-1}. The particulate suspensions (*E. coli*, spores, or fluospheres) were aerosolized and collected in a seven-stage Ultimate cascade impactor (35). A microscope slide thinly coated with 5% (vol/vol) gelatin was placed at each stage to collect the particles. The length of spray time was restricted to 5 s to prevent the coagulation of particles observed at higher spray times. The impacted particles leave an impression in the gelatin proportional to the original diameter of the particle. Only particles of a defined size range, from >1 to <32 μm, were collected on each of the seven stages. The slides were analyzed by use of an Olympus IX70 inverted laser confocal microscope (Olympus, Germany) under ×60 water immersion. The fluorescent samples were excited at 488 nm and detected using either a 530-nm band-pass filter (FITC, fluorescein, green FluoSpheres) or a 565-nm long-pass filter (red FluoSpheres). Images were recorded and processed using a Fluoview imaging system (Olympus, Germany). On each slide, at least 200 particles were counted from 20 fields of view. The number of particulates contained within each particle was recorded. The diameter of the original particles prior to impaction into the gelatin was derived (in micrometers) from the scale provided by the imaging software. The actual size of the original particle was obtained by multiplication of the diameter of the impacted particle by a conversion factor of 0.59 (33). All experiments were performed in triplicate.

Determination of the effect of aerosolization on bacterial viability. *E. coli* MRE162 was cultured to a density of $2.2 \times 10^9 \pm 0.13 \times 10^9$ CFU ml^{-1} in nutrient broth and split into equal 10-ml volumes for aerosolization using the Collison nebulizer or the FFAG for 1, 2, or 5 min. The aerosols were collected on fresh Whatman glass microfiber filters (grade GF/A, 47-mm diameter; Sigma-Aldrich Ltd., United Kingdom) by drawing compressed air through at a flow rate of 66 liters min^{-1}. Immediately after collection, the filters were placed into 5 ml of PBS and vigorously shaken for 30 s to remove the deposited bacteria. Enumeration was done by serial dilution and spread plating of 100-μl aliquots in triplicate onto nutrient agar plates. The plates were incubated for 24 h at 37°C. The percent survival was calculated by dividing the number of bacteria obtained after aerosolization by the number of bacteria present preaerosolization. The resultant value was multiplied by 100 to derive the percentage.

Determination of site of deposition within the murine model. Mice were nose-only exposed for 10 min to aerosols containing either *E. coli* MRE162 or FluoSpheres by use of the FFAG or the Collison nebulizer. The exposures were maintained at a constant temperature of 20 ± 0.5°C. The respiratory volume was obtained from Guyton's formula (20), and the retained dose was calculated via the method of Harper and Morton (21). The actual inhaled dose was derived from the nasal washes and dissected lungs, tracheae, esophagi, and stomachs

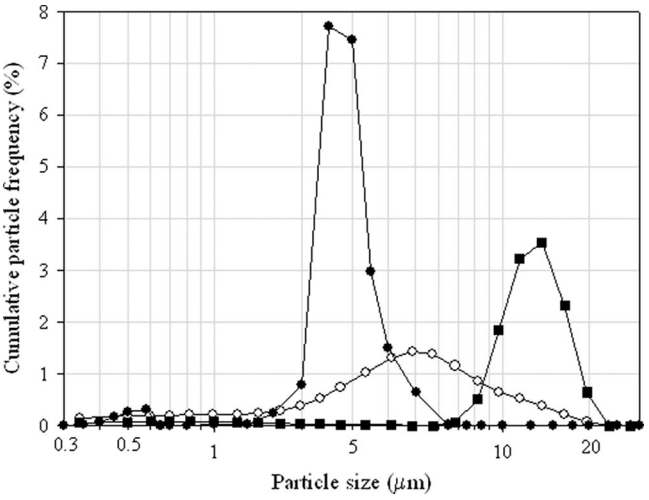

FIG. 1. Representative mass distributions for the Collison nebulizer and the FFAG at the points of generation and inhalation. ○, Collison nebulizer, preinhalation (MMAD of 3.84 μm, GSD of 2.12); ●, Collison nebulizer, inhaled (MMAD of 2.51 μm, GSD of 1.28); ■, FFAG, preinhalation and inhaled (MMAD of 12.63 μm, GSD of 1.35).

from sacrificed mice. For each particulate, 10 mice were challenged with either large- or small-particle aerosols. Immediately after exposure, the mice were culled by irreversible anesthesia via intraperitoneal administration of 0.5 ml sodium pentobarbital. The respiratory tracts and digestive tracts were aseptically dissected. Nasal washes were collected by inserting a catheter (outer and inner diameters of 1.02 and 0.58 mm, respectively, and length of 40 mm; Harvard Apparatus Ltd., United Kingdom) into a small incision made in the trachea; the deposited materials in the nasal passages were washed out through the nostrils by use of 1 ml of PBS solutions containing final concentrations of 1 mM NaOH and 0.1% (vol/vol) Triton X-100. The lungs, trachea, esophagus, and stomach were removed and homogenized in PBS through a 0.1-μm cell strainer (VWR International, United Kingdom) by using the plunger from a disposable 2-ml syringe (VWR International, United Kingdom). Enumeration of bacterial counts was done by serial dilution and spread plating 100-μl aliquots in triplicate onto nutrient agar plates. The concentration of FluoSpheres within the homogenized tissue samples was determined by comparison against a standard curve of homogenized tissue samples spiked with known concentrations ranging from 10^2 to 10^8 FluoSpheres ml^{-1}. Fluorescence was detected using a spectrofluorometer (excitation wavelength of 488 nm, emission wavelength of 520 nm; Molecular Devices, CA). Data were acquired and assimilated using SOFTmaxPRO software (Molecular Devices, CA).

Statistical analysis. Aerosol distribution data are expressed as the standard errors of the means from either three or five replicate experiments. A paired *t* test was used for comparison between groups by use of the MiniTab Release 14 version 02 statistical package.

RESULTS

The Collison nebulizer and the FFAG generate aerosols with different mass distributions. To ascertain whether the Collison nebulizer and the FFAG produce distinctive aerosols, they were compared with respect to mass distribution. The aerosols generated at the exit orifice of the devices and within the exposure tube where the mice inhale the aerosols were compared (Fig. 1). The aerosol generated by the FFAG demonstrated an MMAD of 12.63 μm, with a particle distribution ranging from 8 to 20 μm. This was irrespective of whether measurement of the distribution occurred at the exit orifice or within the exposure tube. The aerosol generated by the FFAG was maintained at 65 to 70% RH to minimize evaporation within the exposure tube. In contrast, the mass distributions obtained for the Collison nebulizer differed depending on whether the aerosol was sampled at the exit orifice of the device or within the exposure tube. The aerosol generated at the orifice of the Collison nebulizer had an MMAD of 3.84 μm, with a range of 0.5 to 20 μm. The distribution obtained within the exposure tube for the Collison nebulizer shifted to an MMAD of 2.51 μm, with a range of 1 to 7 μm. In the cases of both the FFAG and the Collison nebulizer, the aerosols measured at the top, midpoint, and bottom of the exposure tube were identical (data not shown).

Particle size distributions of bacteria and spores generated by the FFAG and Collison nebulizer differ. The number of entrapped particulates within the individual particles of an aerosol is an important characteristic that is relevant for dispersion, infectivity, and survival of the incorporated microbes. As the size of the particles within an aerosol increases, it is likely that the number of entrapped particulates increases accordingly. Three different particulates (bacteria, spores, and FluoSpheres) were investigated with respect to distribution within the aerosol particles generated by the Collison nebulizer or the FFAG (Table 1; Fig. 2). The trends for all three particulates were similar. Independently of the particulate type, the number of particulates entrapped within the particles generated by the FFAG increased as the particle size increased from 0 to 3 μm to 3 to 9 μm to 9 to 17 μm. Greater numbers of spores and *E. coli* cells than FluoSpheres were contained within the large particles (9 to 17 μm) produced by the FFAG. Independently of particulate type, the 9- to 17-μm particles generated by the FFAG contained numbers of entrapped particulates significantly greater than those generated by the Collison nebulizer (15.9- to 19.2-fold; $P = 0.001$). The fact that, compared to FluoSpheres, a large number of *E. coli* and *B. atrophaeus* spores were entrapped as a function of particle size was probably due to a combination of the reduced volume of bacteria and spores and their greater tendency to aggregate (Fig. 3). The FFAG generated fewer 1- to 3-μm particles than

TABLE 1. Effect of particulate type on the number incorporated per particle size fraction for the Collison nebulizer and the FFAG[a]

Particle size fraction (μm)	Avg[b] no. (±SE) of particulates per particle					
	Fluospheres		*B. atrophaeus* spores		*E. coli*	
	Collison	FFAG	Collison	FFAG	Collison	FFAG
0–3	0.82 ± 0.01	0.47 ± 0.02	1.06 ± 0.05	0.80 ± 0.04	0.91 ± 0.03	0.49 ± 0.02
4–8	0.13 ± 0.02	3.31 ± 0.18	1.45 ± 0.08	3.08 ± 0.62	0.87 ± 0.06	5.11 ± 0.12
9–17	0.39 ± 0.07	7.09 ± 0.29	2.80 ± 0.40	53.82 ± 8.64	0.92 ± 0.04	14.67 ± 0.55

[a] Particulates were aerosolized from distilled water at a concentration of 10^9 ml^{-1} at a flow rate of 50 μl min^{-1} and a pressure of 16 lb/in^2 (110,000 Pa).
[b] Averages were derived from five representative experiments.

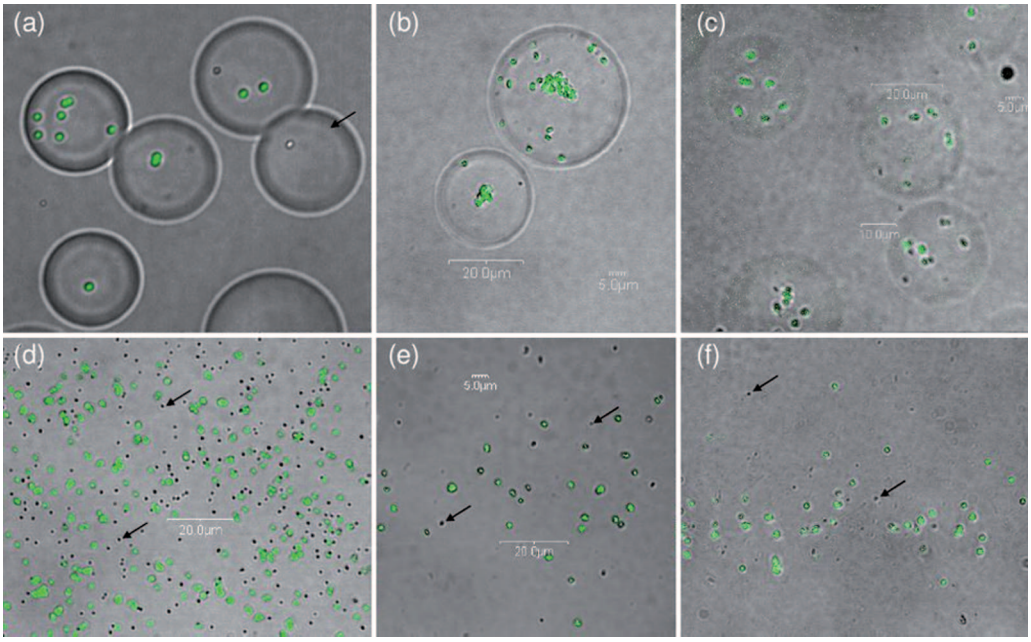

FIG. 2. Representative confocal microscopic images of particles collected in the Ultimate cascade impactor from an aerosol (12-μm MMAD) generated by the FFAG containing FluoSpheres (a and d), *B. atrophaeus* spores (b and e), or *Escherichia coli* MRE162 cells (c and f). The imaged particles are 8 to 16 μm (a, b, and c) or 1 to 2 μm (d, e, and f). Particulates were aerosolized at a concentration of 10^9 ml^{-1}. Arrows indicate empty particles.

the Collison nebulizer (Fig. 1). Significantly more of the 1- to 3-μm particles generated by the Collison nebulizer than by the FFAG contained particulates (82 to 106 and 47 to 80%, respectively; $P = 0.002$). Empty 1- to 3-μm particles can clearly be observed in the aerosol generated by the FFAG (Fig. 2d, e, and f).

Bacteria in particles generated using the FFAG survive better in the aerosol state. The culturability of *E. coli* was assessed after aerosolization for 1, 2, and 5 min with the Collison nebulizer and the FFAG (Fig. 4). Over the first minute of operation, the numbers of culturable bacteria recovered decreased markedly for both the Collison nebulizer (71.82% ± 4.82%) and the FFAG (94.66% ± 2.59%). Thereafter, the rate of decrease in survival was significantly greater for the Collison nebulizer than for the FFAG ($P > 0.5$).

Particle size affects the site of deposition within the murine inhalational model. To confirm the utility of the FFAG as a generator of large-particle aerosols, the FFAG was compared with the Collison nebulizer with respect to deposition profile within the murine respiratory tract, using both *E. coli* and FluoSpheres as the particulates (Fig. 5). The mass distributions obtained with the Grimm particle analyzer showed MMADs of 12.11 and 12.36 μm for *E. coli* and FluoSpheres, respectively, aerosolized by the FFAG. Within the respiratory tract, the 1- to 3-μm particles containing *E. coli* generated by the Collison nebulizer preferentially deposited in the lungs as opposed to the nasal passages (6.49×10^3 and 5.39×10^2 CFU ml^{-1}, respectively; $P = 0.05$). Significant quantities of the aerosolized materials were found in the esophagus and stomach (89.7%). In contrast, the 12-μm particles generated by the FFAG pref-

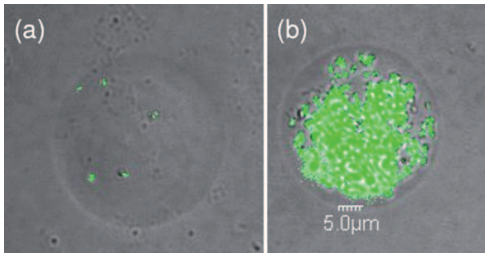

FIG. 3. Representative confocal microscopic images of (a) normally and (b) extremely loaded 12-μm particles collected in the Ultimate cascade impactor from an aerosol generated by the FFAG containing *B. atrophaeus* spores. Particulates were aerosolized in distilled water at a concentration of 10^9 ml^{-1}.

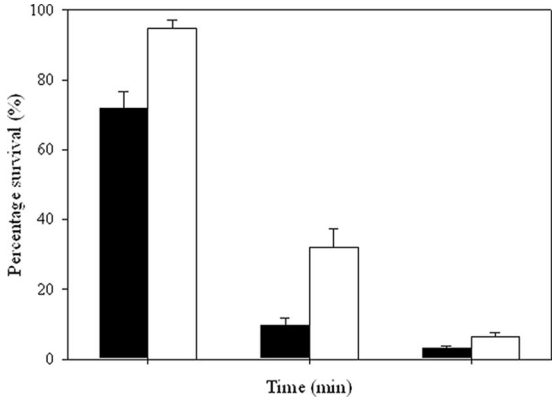

FIG. 4. Comparative survival of *E. coli* MRE162 cells after aerosolization. Black and white bars represent depositions of the Collison nebulizer and the FFAG, respectively. Averages were derived from three representative experiments.

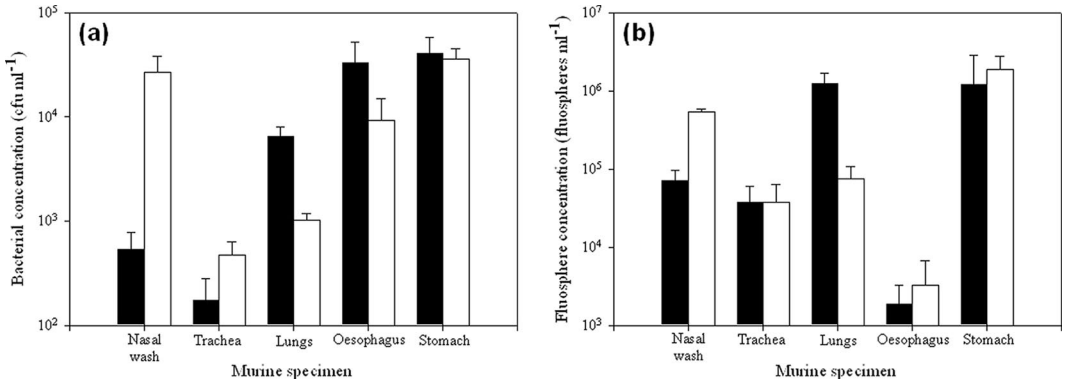

FIG. 5. Deposition in the murine model of aerosols generated by the Collison nebulizer and the FFAG containing (a) *E. coli* MRE162 and (b) FluoSpheres. Black and white bars represent deposition of the Collison nebulizer and the FFAG, respectively. Distribution data are as follows: for distilled water, MMAD of 12.36 μm and GSD of 1.38; for *E. coli*, MMAD of 12.11 μm and GSD of 1.33; and for FluoSpheres, MMAD of 12.36 μm and GSD of 1.39. Particulates were sprayed at a concentration of 10^9 ml^{-1}. Error bars represent the standard errors of the means ($n = 10$).

erentially deposited in the nasal passages as opposed to the lungs (2.67×10^4 and 1.03×10^3 CFU ml^{-1}, respectively; $P = 0.06$). Similarly, significant clearance to the esophagus and stomach was observed (61.5%). In both cases, deposition in the trachea was minimal. Similar trends were observed for fluospheres, where greater deposition in the lungs than in the nasal passages was observed for the aerosol generated by the Collison nebulizer ($P = 0.001$); the reverse was evident for the FFAG, with greater deposition of FluoSpheres in the nasal passages than in the lungs ($P = 0.001$). For both *E. coli* and FluoSpheres, significant differences in the concentrations of material deposited in the lungs compared to the nasal passages were observed ($P < 0.5$).

DISCUSSION

The ability to assess both small- and large-particle microbiological aerosols in relation to infection was developed during the 1950s and 1970s. These studies used the STAG to generate large-particle aerosols in the range of 1- to 20-μm dried particles (9, 10, 11, 12, 21), while the Collison nebulizer was used to produce the small-particle aerosols (34). The STAG was recently used to deposit large particles containing ricin within the murine URT; however, the distribution achieved was bimodal, with peaks at 5 and 12 μm (43). Therefore, deposition solely within the URT was not achieved. Recently, the phenomenon of flow focusing, which generates monodisperse aerosols with MMADs greater than 10 μm, was described (16, 17, 31). These studies represent the first investigation of flow focusing as a novel mechanism for the experimental aerosolization of microbes and application to the delivery of microbial aerosols to an animal model.

An important consideration regarding deposition within the respiratory tract is the sizes of particles inhaled by the animals during exposure rather than present at the point of production by the device. Two profiles were obtained for the Collison nebulizer, corresponding to the distributions generated at the orifice of the device and at the point the animals inhaled the aerosol. Previous analysis of the particles produced at the orifice of the Collison nebulizer indicated a range of 0.25 to 25 μm (34). In this study, the mass distribution of the aerosol generated by the Collison nebulizer at the orifice was a close parallel. However, the aerosol that the mice inhaled was in the 1- to 5-μm range, due to evaporation within the Henderson apparatus at 45 to 50% RH. If evaporation of the 12-μm particles occurred during travel from the point of production to the animals' noses, then the particle distribution inhaled and hence the deposition profile would be altered significantly. Evaporation of the 12-μm-particle aerosol produced by the FFAG is prevented by feeding the aerosol directly into the exposure tube at 65 to 70% RH. Therefore, the aerosol to which the animals are exposed is identical to that generated at the orifice of the FFAG. Hence, within the exposure tube, the aerosol generated by the Collison nebulizer comprised a significantly greater number of smaller particles (1 to 5 μm), while the aerosol generated by the FFAG contained a greater number of larger particles (10 to 15 μm). The Collison nebulizer and the FFAG produced different mass distribution profiles, which enables the effect of particle size on deposition within the lower and upper respiratory tracts to be determined (Fig. 5).

The relationship of particulate number to particle size is important because it impacts the number of particles required to be inhaled to initiate infection (i.e., the lethal dose) or the quantity of material that can be deposited on surfaces. As 12-μm particles contain greater numbers of bacteria or spores than do 1-μm particles, it is evident that fewer particles need to be inhaled to reach the lethal dose and initiate infection. This is of course subject to the proviso that differential regional depositions within the respiratory tract due to particle size do not alter disease kinetics and severity. The volume of a spherical particle with a 12-μm diameter is 904.78 μm^3. Assuming ellipsoidal morphology, the volumes of *B. atrophaeus* spores and *E. coli* cells have been determined as 0.273 ± 0.046 μm^3 (5) and 0.33 μm^3 (length of 1.4 to 1.6 μm; diameter of 0.65 ± 0.04 μm) (52), respectively. The number of unit spheres (particulates) that can be packaged into a larger volume (particle) is determined by sphere packing theory. Due to the rigidity of the spheres, the larger volume will not be filled because spaces occur between spheres, requiring consideration of fractional filling volume. Two packing arrangements permit the densest packaging of small spheres (particulates) into lattices within

larger spheres (particles) with a fractional filling volume of 0.7405: face centered cubic and hexagonal close packing (7, 30). Hence, the maximum calculated numbers of *E. coli* cells, *B. atrophaeus* spores, or FluoSpheres packaged within a 12-μm particle are 2,030, 2,454, and 961, respectively. The actual particulate numbers observed were much lower (Table 1; Fig. 2), probably because a large portion of the matrix of the particle comprised the suspending medium from which the aerosol was derived. Due to aggregation, higher numbers of particulates were observed, particularly for *B. atrophaeus* spores (Fig. 3) but also occasionally for *E. coli* cells. Inhalation of these particles may have a significant effect on disease outcome and warrant consideration.

The survival of bacteria during the initial process of aerosolization in the apparatus will influence survival during extended aerosolization and thus infection upon deposition in the respiratory tract. Initially, mechanical and shear stresses are imparted by the actual act of aerosol generation within the device. Thereafter, bacteria are rapidly inactivated in situ due to a number of environmental stresses, including desiccation and UV radiation (27, 49, 50). In this study, temporally dependent significant differences between the numbers of culturable *E. coli* cells collected on filters after aerosolization by the Collison nebulizer and by the FFAG were observed (Fig. 4). It is currently unclear whether the increased survival observed with *E. coli* aerosolized by the FFAG was due to differential survival resulting from incorporation into larger particles or due to the reduced mechanical stress imparted during flow focusing. Interestingly, bacterial survival has been related to particle size. Bacteria survived better within 7-μm particles than within 1.1-μm particles, as a function of temperature, RH, and solar radiation (28, 50). This phenomenon is proposed to be due to larger particles containing higher numbers of bacteria in aggregates, enabling a fraction to survive deleterious stresses encountered during aerosolization. The outer layer of bacteria effectively is sacrificial, enabling the bacteria within the core of the aggregate to survive (4, 28); such aggregation of *B. atrophaeus* spores was observed in this study (Fig. 3). An interesting aspect of bacterial physiology not investigated in this study is the phenomenon of bacterial injury and the formation of "viable but nonculturable" cells during aerosolization (22, 44, 48). The physiological status of aerosolized bacteria may play an important role in aerosol survival, persistence, and, subsequently, infection with respiratory pathogens, and research to investigate this phenomenon with respect to particle size is under way.

The overall deposition trends for the aerosols generated by the Collison nebulizer and the FFAG are similar to previously published data in the murine model, although the CF1 strain was used rather than the BALB/c strain (41). For 1.09-μm particles, the fractions deposited in the lungs (pulmonary and bronchial), trachea, URT (skull and larynx), and GI tract were 26.4, 0.3, 8.6, and 64.7%, respectively. In this study, for the Collison nebulizer (1- to 3-μm particles), the fractions deposited in the lungs, trachea, URT, and GI tract were 8.04, 0.21, 0.67, and 89.7%, respectively. The general trends of greater deposition in the lungs than in the URT were similar in both studies, although much greater clearance to the esophagus and stomach was observed in this study. In comparison, for 9.65-μm particles, the fractions deposited in the lungs, trachea, URT, and GI tract were 0.44, 0.26, 74.8, and 24.5%, respectively (41). In this study, for the FFAG (10- to 15-μm particles), the fractions deposited in the lungs, trachea, URT, and GI tract were 1.4, 0.64, 36.5, and 61.5%, respectively. To our knowledge, this study represents the first description of the deposition of an aerosol comprising predominantly 12-μm particles within the murine respiratory tract. Differences between the two studies may in part be due to intraspecies anatomical and physiological differences; for example, BALB/c and $B6C3F_1$ mice possess significant differences in airway anatomy, correlating with differences in body length and chest circumference (38, 39). A significant portion of the deposited material was cleared to the GI tract, possibly via epithelial mucociliary clearance mechanisms in some areas of the nasal passages and the tracheobronchial system. In the murine model (strain C57BL/6), clearance rates from the mucociliary escalators are rapid, at 2.2 ± 0.45 mm min^{-1} and 1.3 ± 0.26 mm min^{-1} for the trachea and nasal passages, respectively (18). The quantity of deposited bacteria cleared to the GI tract raises the important question of whether an inhalational challenge could result in "dual" infection of both the respiratory region and the GI tract. This would depend on microbial survival of the physical defense mechanisms in the stomach and intestine, including pH extremes and enzymatic degradation.

In conclusion, the FFAG is capable of delivering large-particle aerosols in the region of 12 μm to the nasal passages of the murine model within BSL-3 containment. The aerosol generated differs significantly from that produced by the Collison nebulizer with respect to mass distribution, distribution of particulates within the particles, and deposition within the murine respiratory tract. Flow-focusing technology has the potential to be utilized for the investigation of aerobiological research topics within diverse areas of applied microbiology, such as agriculture, food processing, water, biodefense, and health care industries. The ability to preferentially deposit pathogens within different regions of the respiratory tract will permit analysis of disease kinetics with respect to particle size. Future work will utilize the two aerosol generators to characterize the infections generated by differential deposition of aerosolized bacteria to the lungs or URT.

ACKNOWLEDGMENTS

We recognize the contribution of Ministry of Defense funding for this research.

Special thanks are reserved for the personnel involved in the animal husbandry related to completion of the experiments.

REFERENCES

1. **Bémer, D., J. Fismes, I. Subra, V. Blachère, and J.-C. Protois.** 2007. Pesticide aerosol characteristics in the vicinity of an agricultural vehicle cab during application. J. Occup. Environ. Hyg. **4:**476–482.
2. **Bollin, G. E., J. F. Plouffe, M. F. Para, and B. Hackman.** 1985. Aerosols containing *Legionella pneumophila* generated by shower heads and hot-water faucets. Appl. Environ. Microbiol. **50:**1128–1131.
3. **Borio, L., D. Frank, V. Mani, C. Chiriboga, M. Pollanen, M. Ripple, S. Ali, C. DiAngelo, J. Lee, J. Arden, J. Titus, D. Fowler, T. O'Toole, H. Masur, J. Bartlett, and T. Inglesby.** 2001. Death due to bioterrorism-related inhalational anthrax: report of 2 patients. JAMA **286:**2554–2559.
4. **Carrera, M., J. Kesavan, R. Zandomeni, and J.-L. Sagripanti.** 2005. Method to determine the number of bacterial spores within aerosol particles. Aerosol Sci. Technol. **39:**960–965.
5. **Carrera, M., R. O. Zandomeni, J. Fitzgibbon, and J.-L. Sagripanti.** 2007. Difference between the spore sizes of *Bacillus anthracis* and other *Bacillus* species. J. Appl. Microbiol. **102:**303–312.
6. **Cole, E. C., and C. E. Cook.** 1998. Characterization of infectious aerosols in

healthcare facilities: an aid to effective engineering controls and preventative strategies. Am. J. Infect. Control **26:**453–464.
7. **Conway, J. H., and N. J. A. Sloane (ed.).** 1993. Sphere packings, lattices, and groups. New Springer Verlag, New York, NY.
8. **Donaldson, A. I., and S. Alexandersen.** 2002. Predicting the spread of foot and mouth disease by airborne virus. Rev. Sci. Tech. **21:**569–575.
9. **Druett, H. A., and K. R. May.** 1952. A wind tunnel for the study of airborne infections. J. Hyg. **50:**69–81.
10. **Druett, H. A., D. W. Henderson, L. P. Packman, and S. Peacock.** 1953. Studies on respiratory infection I. The influence of particle size on respiratory infection with anthrax spores. J. Hyg. **51:**359–371.
11. **Druett, H. A., J. M. Robinson, D. W. Henderson, L. Packman, and S. Peacock.** 1956. Studies on respiratory infection II. The influence of aerosol particle size on infection of the Guinea-pig with *Pasteurella pestis.* J. Hyg. **54:**37–48.
12. **Druett, H. A., D. W. Henderson, and S. Peacock.** 1956. Studies on respiratory infection III. Experiments with *Brucella suis.* J. Hyg. **54:**49–57.
13. **Duan, H.-Y., T. Chai, Y. Cai, Z.-B. Zhong, M. Yao, and X.-X. Zhang.** 2008. Transmission identification of *Escherichia coli* aerosol in chicken houses to their environments using ERIC-PCR. Sci. China C **51:**164–173.
14. **Fennelly, K. P., J. W. Martyny, K. E. Fulton, I. M. Orme, D. M. Cave, and L. B. Heifets.** 2004. Cough-generated aerosols of *Mycobacterium tuberculosis.* A new method to study infectiousness. Am. J. Respir. Crit. Care Med. **169:**604–609.
15. **Fung, F., and W. G. Hughson.** 2003. Health effects of indoor fungal bioaerosol exposure. Appl. Occup. Environ. Hyg. **18:**535–544.
16. **Gañan-Calvo, A. M.** 1998. Generation of steady liquid microthreads and micron-sized monodisperse sprays in gas streams. Phys. Rev. Lett. **80:**285–288.
17. **Gañan-Calvo, A. M., and A. Barrero.** 1999. A novel pneumatic technique to generate steady capillary microjets. J. Aerosol Sci. **30:**117–125.
18. **Grubb, B. R., J. H. Jones, and R. C. Boucher.** 2004. Mucociliary transport determined by *in vivo* microdialysis in the airways of normal and CF mice. Am. J. Physiol. Lung Cell. Mol. Physiol. **286:**588–595.
19. **Gustavsson, P., and E. Borch.** 1993. Contamination of beef carcasses by psychrotrophic *Pseudomonas* and *Enterobacteriaceae* at different stages along the processing line. Int. J. Food Microbiol. **20:**67–83.
20. **Guyton, A.** 1947. Measurement of the respiratory volumes of laboratory animals. Am. J. Physiol. **150:**70–77.
21. **Harper, G. J., and J. D. Morton.** 1953. The respiratory retention of bacterial aerosols: experiments with radioactive spores. J. Hyg. **51:**372–385.
22. **Heidelberg, J. F., M. Shahamat, M. Levin, I. Rahman, G. Stelma, C. Grim, and R. R. Colwell.** 1997. Effect of aerosolization on culturability and viability of gram-negative bacteria. Appl. Environ. Microbiol. **63:**3585–3588.
23. **Henderson, D. W.** 1952. An apparatus for the study of airborne infection. J. Hyg. **50:**53–68.
24. **Heyder, J., J. Gebhart, G. Rudolf, C. F. Schiller, and W. Stahlhofen.** 1986. Deposition of particles in the human respiratory tract in the size range 0.005–15 μm. J. Aerosol Sci. **17:**811–825.
25. **Knight, V.** 1980. Viruses as agents of airborne contagion. Ann. N. Y. Acad. Sci. **353:**147–156.
26. **Laumbach, R. J., and H. M. Kipen.** 2005. Bioaerosols and sick building syndrome: particles, inflammation, and allergy. Curr. Opin. Allergy Clin. Immunol. **5:**135–139.
27. **Lighthart, B.** 1997. The ecology of bacteria in the alfresco atmosphere. FEMS Microbiol. Ecol. **23:**263–274.
28. **Lighthart, B., and B. T. Shaffer.** 1997. Increased airborne bacterial survival as a function of particle content and size. Aerosol Sci. Technol. **27:**439–446.
29. **Lippmann, M., and R. E. Albert.** 1969. The effect of particle size on the regional deposition of inhaled aerosols in the human respiratory tract. Am. Ind. Hyg. Assoc. J. **30:**257–275.
30. **Martin, I., B. Dozin, R. Quarto, R. Cancedda, and F. Beltrame.** 1997. Computer-based technique for cell aggregation analysis and cell aggregation in *in vitro* chondrogenesis. Cytometry **28:**141–146.
31. **Martin-Banderas, L., M. Flores-Mosquera, P. Riesco-Cheuca, A. Rodriguez-Gil, A. Cebolla, S. Chavez, and A. M. Gañan-Calvo.** 2005. Flow focusing: a versatile technology to produce size-controlled and specific-morphology microparticles. Small **1:**688–692.
32. **May, K. R., and G. J. Harper.** 1957. The efficiency of various liquid impinger samplers in bacterial aerosols. Br. J. Ind. Med. **14:**287–297.
33. **May, K. R.** 1959. Detecting volatile airborne droplets. Nature **183:**742–743.
34. **May, K. R.** 1973. The Collison nebulizer: description, performance and application. J. Aerosol Sci. **4:**235–243.
35. **May, K. R.** 1975. An "Ultimate" cascade impactor for aerosol assessment. J. Aerosol Sci. **6:**413–419.
36. **Menache, M., F. Miller, and O. Raabe.** 1995. Particle inhalability curves for humans and small laboratory animals. Ann. Occup. Hyg. **39:**317–328.
37. **Nicas, M., W. W. Nazaroff, and A. Hubbard.** 2005. Toward understanding the risk of secondary airborne infection: emission of respirable pathogens. J. Occup. Environ. Hyg. **2:**143–154.
38. **Oldham, M. J., and R. F. Phalen.** 2002. Dosimetry implications of upper tracheobronchial airway anatomy in two mouse varieties. Anat. Rec. **268:**59–65.
39. **Phalen, R. F., M. J. Oldham, and R. K. Wolff.** 2008. The relevance of animal models for aerosol studies. J. Aerosol Med. **21:**1–12.
40. **Posch, J., G. Feierl, G. Wuest, W. Sixl, S. Schmidt, D. Haas, F. F. Reinthaler, and E. Marth.** 2006. Transmission of *Campylobacter* spp. in a poultry slaughterhouse and genetic characterisation of the isolates by pulsed-field gel electrophoresis. Br. Poult. J. **47:**286–293.
41. **Raabe, O. G., M. A. Al-Bayati, S. V. Teague, and A. Raslot.** 1988. Regional deposition of inhaled monodisperse coarse and fine aerosol particles in small laboratory animals. Ann. Occup. Hyg. **32:**53–63.
42. **Rothman, T., and J. O. Ledbetter.** 1975. Droplet size of cooling tower fog. Environ. Lett. **10:**191–203.
43. **Roy, C. J., M. Hale, J. M. Hartings, and L. Pitt.** 2003. Impact of inhalation exposure modality and particle size on the respiratory deposition of ricin in Balb/c mice. Inhal. Toxicol. **15:**619–638.
44. **Rule, A. M., J. Kesavan, K. J. Schwab, and T. J. Buckley.** 2007. Application of flow cytometry for the assessment of preservation and recovery efficiency of bioaerosol samplers spiked with *Pantoea agglomerans.* Environ. Sci. Technol. **41:**2467–2472.
45. **Schlesinger, R. B.** 1985. Comparative deposition of inhaled aerosols in experimental animals and humans: a review. J. Toxicol. Environ. Health **15:**197–214.
46. **Tang, J. W., Y. Li, I. Fames, P. K. Chan, and G. L. Ridgway.** 2006. Factors involved in the aerosol transmission of infection and control of ventilation in healthcare premises. J. Hosp. Infect. **64:**100–114.
47. **Tellier, R.** 2006. Review of aerosol transmission of influenza A virus. Emerg. Infect. Dis. **12:**1657–1662.
48. **Terzieva, S., J. Donnelly, V. Ulevicius, S. A. Grinshpun, K. Willeke, G. N. Stelma, and K. P. Brenner.** 1996. Comparison of methods for detection and enumeration of airborne microorganisms collected by liquid impingement. Appl. Environ. Microbiol. **62:**2264–2272.
49. **Tong, Y., and B. Lighthart.** 1997. Solar radiation has a lethal effect on natural populations of culturable outdoor atmospheric bacteria. Atmos. Environ. **31:**897–900.
50. **Tong, Y., and B. Lighthart.** 1998. Effect of simulated solar radiation on mixed outdoor atmospheric bacterial populations. FEMS Microbiol. Ecol. **26:**311–316.
51. **Wells, W. F.** 1934. On air-borne infection. Study II. Droplets and droplet nuclei. Am. J. Hyg. **20:**611–618.
52. **Woldringh, C. L., M. A. de Jong, W. van den Berg, and L. Koppes.** 1977. Morphological analysis of the division cycle of two *Escherichia coli* substrains during slow growth. J. Bacteriol. **131:**270–279.
53. **Zhou, Y., J. M. Benson, C. Irvin, H. Irshad, and Y.-S. Cheng.** 2007. Particle size distribution and inhalation dose of shower water under selected operating conditions. Inhal. Toxicol. **19:**333–342.